Precambrian Research 246 (2014) 54–63

Contents lists available at ScienceDirect

Precambrian Research

journal homepage: www.elsevier.com/locate/precamres

$^{40}Ar/^{39}Ar$ dating of exceptional concentration of metals by weathering of Precambrian rocks at the Precambrian–Cambrian boundary

John Parnell[a,*], Darren F. Mark[b], Robert Frei[c,d], Anthony E. Fallick[b], Rob M. Ellam[b]

[a] School of Geosciences, University of Aberdeen, Aberdeen AB24 3UE, UK
[b] Isotope Geosciences Unit, Scottish Universities Environmental Research Centre (SUERC), Scottish Enterprise Park, Rankine Avenue, East Kilbride G75 0QF, UK
[c] Department of Geology and Natural Resource Management, Geology Section, University of Copenhagen, Øster Voldgade 10, 1350 Copenhagen, Denmark
[d] Nordic Center for Earth Evolution, NordCEE, Copenhagen, Denmark

ARTICLE INFO

Article history:
Received 6 December 2013
Received in revised form 24 February 2014
Accepted 26 February 2014
Available online 12 March 2014

Keywords:
Precambrian
Precambrian–Cambrian boundary
Great unconformity
Ore deposits
Weathering
Metazoan

ABSTRACT

The sub-Cambrian surface, including diverse metalliferous deposits, shows evidence of intense weathering of Precambrian rocks to form supergene-enriched ores and metalliferous placers, followed by widespread peneplanation. Much of the metal would have been flushed to the Cambrian ocean during peneplanation. An $^{40}Ar/^{39}Ar$ age of 542.62 ± 0.38 Ma (1 sigma, full external precision, Renne et al., 2011) for metalliferous alteration clays in Scotland shows that this event occurred immediately prior to the Precambrian–Cambrian boundary. A negative $\delta^{53}Cr$ isotopic signature for the clay is consistent with mobilization on land of redox sensitive metals by oxidative terrestrial weathering. This unprecedented flushing of metals from the weathered Precambrian surface would have contributed to the chemistry of the earliest Cambrian ocean at a time of marked faunal evolution.

1. Introduction

The Precambrian–Cambrian boundary marks one of the most dramatic episodes of change in Earth's history. The evolution and diversification of metazoans accelerated following a mass extinction, while ocean geochemistry was transformed globally. The temporal association has been interpreted to indicate a genetic link between geochemical change and faunal evolution (Amthor et al., 2003; Wille et al., 2008; Maloof et al., 2010; Peters and Gaines, 2012). Geochemical change at the boundary is evident as metal enrichment (Schrödinger and Grotzinger, 2007; Wille et al., 2008), and specifically Rare Earth Element (REE) enrichment (Xu et al., 1989), an iridium anomaly (Nazarov et al., 1983), increase in radiogenic marine strontium (Shields, 2007), and widespread phosphate deposition (Cook, 1992). Overall, the early Cambrian ocean is characterized as highly metalliferous (Lehmann et al., 2007). To understand the anomalous precipitation of metals in the oceans, we should examine the nature of the continental surface from which they would have been derived by erosion and run-off. The Precambrian–Cambrian boundary saw marine transgression across intensely weathered surfaces, which commonly show extensive alteration and related planation to a degree without parallel in the geological record (Fig. 1). Thus a sub-Cambrian altered surface can be traced over much of North America (Ambrose, 1964; Duffin, 1989), across the Pan-African Orogen for 6000 km from Morocco to Oman (Avigad et al., 2005), and over much of the Baltic region (Nielsen and Schovsbo, 2011). In each case, the surface is covered with clay alteration products where they are preserved from the accompanying planation, especially by a Lower Cambrian quartz-rich sandstone.

1.1. Weathered and enriched ore deposits on the sub-Cambrian surface

Investigation of the distribution of metalliferous ore deposits on the sub-Cambrian surface leads to two conclusions. Firstly, there was a relatively high abundance of such deposits, and secondly many of these deposits were demonstrably weathered and even enriched before the subsequent peneplanation and transgression. Unlike many unconformable surfaces, which are developed on older sedimentary rocks, the sub-Cambrian surface is extensively developed on deeply eroded crystalline basement, including a disproportionate volume of granites and pegmatites, and metasedimentary iron formations (Duffin, 1989; Avigad et al., 2005). These

* Corresponding author. Tel.: +44 1224273464.
E-mail address: J.Parnell@abdn.ac.uk (J. Parnell).

http://dx.doi.org/10.1016/j.precamres.2014.02.012
0301-9268/

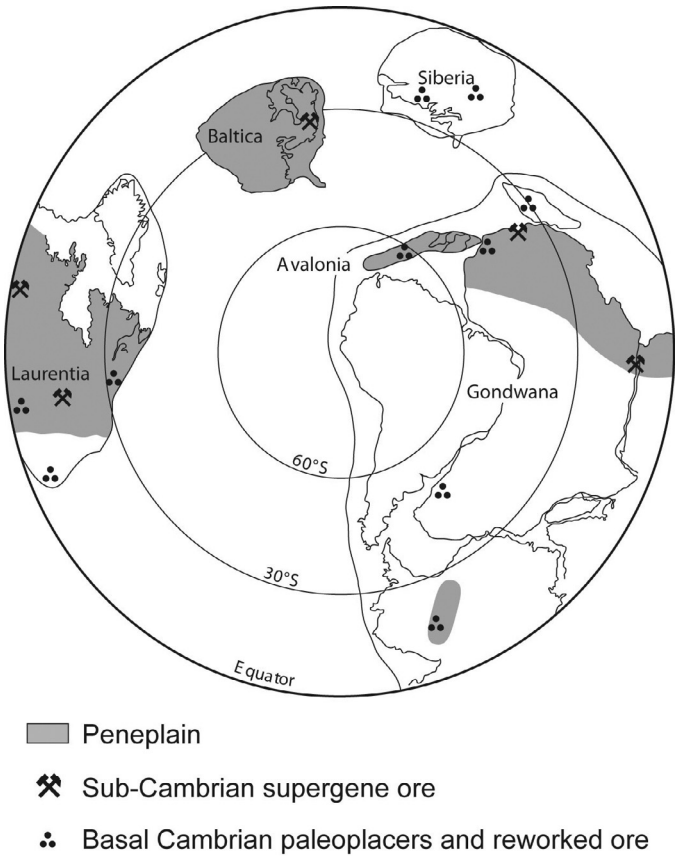

Fig. 1. Palaeogeography for end-Neoproterozoic (~550 Ma) (Torsvik et al., 1996), showing sites for supergene metal enrichment on the sub-Cambrian surface (data sources in text).

rocks are extensively mineralized. Cross-sections through ore deposits in North America in particular commonly show them truncated by the sub-Cambrian unconformity (Fig. 2), but not consistently by any other palaeosurface. This partly reflects the huge area transgressed by the Cambrian ocean. We draw attention to two types of ore on the surfaces that were especially significant to anomalous Cambrian chemistry. Iron deposits were exposed on the surface in many parts of the world, including USA, Canada, Sweden, Iran and West Africa. So much Precambrian iron ore was eroded during the transgression that the basal Cambrian rocks can be ores in their own right, for example, in Missouri and Wyoming (Murphy and Ohle, 1968; Hausel, 1989). Many of these iron deposits are gold-bearing, some are strongly phosphatic, and others contain associated REE deposits. Other types of gold deposit are exposed on the surface, especially in shear zones, for example, in Wyoming (Laurentia), Saskatchewan (Laurentia), Jordan (Gondwana) and Newfoundland (Avalonia) (Bayley et al., 1973; O'Brien, 2002; Saskatchewan Ministry of Energy & Resources, 2008; Al-Hwaiti et al., 2010). In Wyoming there are associated platinum group element ores at the surface, including iridium ore (Hausel, 1989). One of the most important sources of platinum group elements in the world, the Stillwater Complex in Montana, was eroded and exposed at the sub-Cambrian surface (Jackson, 1968). In each case, the ore deposits can be traced up to the sub-Cambrian unconformity (Fig. 3), and so were exposed at the time of peneplanation.

In addition to this evidence of widespread exposure of metalliferous ores on the sub-Cambrian surface, there is evidence for deep weathering and enrichment of the ores. The concentration of metals by weathering could be evident as either supergene enrichment, or the accumulation of palaeoplacers. Supergene alteration and enrichment due to oxidation upgraded the value of the ores before deposition of the Cambrian sediments. Most of the evidence is on the Laurentian continent (Fig. 4), as this has been intensively explored. Examples are supergene concentrations of copper in Wisconsin (May and Dinkowitz, 1996), Michigan (Bornhorst, 2002) and Quebec (Sinclair and Gasparrini, 1980), copper–silver–gold enrichment in Arizona (Schwartz, 1938), iron in Missouri (Emery, 1968), Michigan (James et al., 1968) and Saskatchewan (Cheesman, 1964), nickel enrichment in Manitoba (Cumming and Krstic, 1991), zinc–lead enrichment in New York (Brown, 1936), uranium enrichment in Michigan (Mancuso et al., 1985) and gold enrichment in Ontario (Di Prisco and Springer, 1991). The scale of enrichment is evident in Jerome County, Arizona, where a supergene sub-Cambrian copper ore earned $10 million in 1916 (Lindgren, 1926). In Scotland, which resides on the periphery of the Laurentian continent, supergene chromium minerals are concentrated on the surface, where the Archean gneiss-pegmatite bedrock includes basic layers rich in chromium (see below). Beyond Laurentia, supergene enrichments on the sub-Cambrian surface include copper ores in Morocco and Israel (Gondwana) and lead ores in Norway (Baltica) (Bjørlykke et al., 1990; Asael et al., 2007; Alvaro and Subias, 2011).

Where the weathered surface was eroded to yield an accumulation of resistant minerals, palaeoplacers rich in gold, monazite (rare earths, thorium) and other metalliferous phases became entrained in Cambrian sandstones. Gold-bearing palaeoplacer deposits in Cambrian sandstones occur in Saskatchewan (Rogers, 2011), South Dakota (Paterson et al., 1988), Wyoming (Hausel and Graves, 1996), Texas (Heylmun, 2001), the Yenisey and Anabar regions of the Siberian Platform (Krendelev, 1966; Konstantinovskii, 2001) and Spain (Pérez-García et al., 2000). These concentrations occurred on a vast scale. The Cambrian gold palaeoplacers at the Homestake gold deposit, South Dakota, are estimated at up to a million ounces of gold, while in Wyoming 20 million tonnes of monazite palaeoplacer – rich rock were identified as prospective ore. Together with other Cambrian 'black sand' deposits (heavy mineral palaeoplacers) in Quebec (Gauthier et al., 1994), Namibia (Blanco et al., 2006), Antarctica (Laird, 1981) and Korea (Kim and Lee, 2006), there is global evidence for the concentration of metals on the sub-Cambrian surface that was incorporated into sandstones during the Cambrian transgression. Where the altered sub-Cambrian rock was completely stripped away, the denudation event would have also entrained fresh mineralized rocks. Thus, for example, gold-mineralized late Proterozoic rocks in Newfoundland (Avalonia), copper–silver–mineralized Proterozoic rocks in British Columbia, and Precambrian iron formation in Missouri, Michigan and Saskatchewan (Laurentia), Iran and Mauritania (Gondwana) were all exposed and eroded to supply clasts identified in basal Cambrian deposits (Awmack, 1994; Emery, 1968; O'Brien, 2002; Baldwin and Gross, 1967; Förster and Jafarzadeh, 1994). No comparable concentration and diversity of ore exists on post-Cambrian palaeosurfaces.

2. The sub-Cambrian surface in Scotland

The peneplained surface in NW Scotland is a 'remarkably flat' (Johnstone and Mykura, 1989) surface of Archean gneiss and mid-Proterozoic pegmatites. It is covered by alteration phyllosilicates beneath a protective cover of Lower Cambrian quartz sandstone which extends over a 40 km outcrop (Peach et al., 1907; Russell and Allison, 1985; Allison et al., 1992; Ferguson et al., 1998). X-ray diffraction data show that the cover mineralogy is dominated by pinite, a very fine-grained form of the potassium mica muscovite, which can form from meteoric fluids (Allison et al., 1992). The fine-grained mica (crystals up to 125 μm) has been interpreted as a weathering product because (i) it tops a profile of

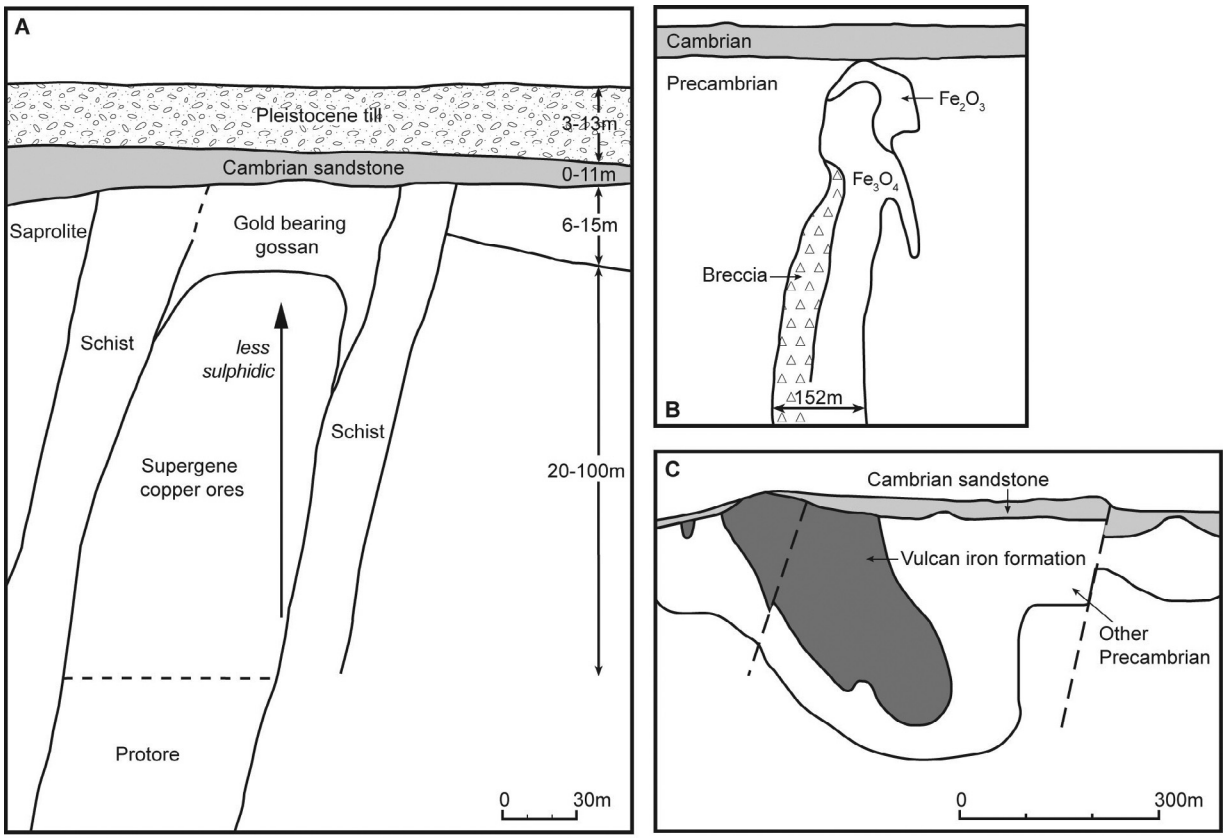

Fig. 2. Cross-sections through Precambrian-hosted ore deposits with supergene alteration below sub-Cambrian unconformity. (A) Flambeau gold–copper deposit, Wisconsin, where gold is enriched below the unconformity (after May and Dinkowitz, 1996); (B) Pea Ridge iron deposit, Missouri, where iron ore is altered from magnetite to haematite below the unconformity (after Emery, 1968); (C) Groveland iron deposit, Michigan, where Cambrian sandstone overlies island of Precambrian iron formation (after Dutton and Zimmer, 1968).

alteration which diminishes downwards (Allison et al., 1992), (ii) there is no evidence of hydrothermal veining, and the hydrothermal minerals which do characterize the Lewisian basement (e.g., epidote) (Johnstone and Mykura, 1989) are completely absent, and (iii) it occurs consistently upon the Lewisian surface over a 40 km distance (Peach et al., 1907).

Precipitation of the pinite by progressive replacement of the bedrock has left patchy remnants of corroded quartz, but other bedrock minerals are mostly destroyed. Unaltered gneiss is rich in feldspars, but they are absent from the altered surface. The gneiss is extensively veined by pegmatites, which are also altered to a mica-quartz mix.

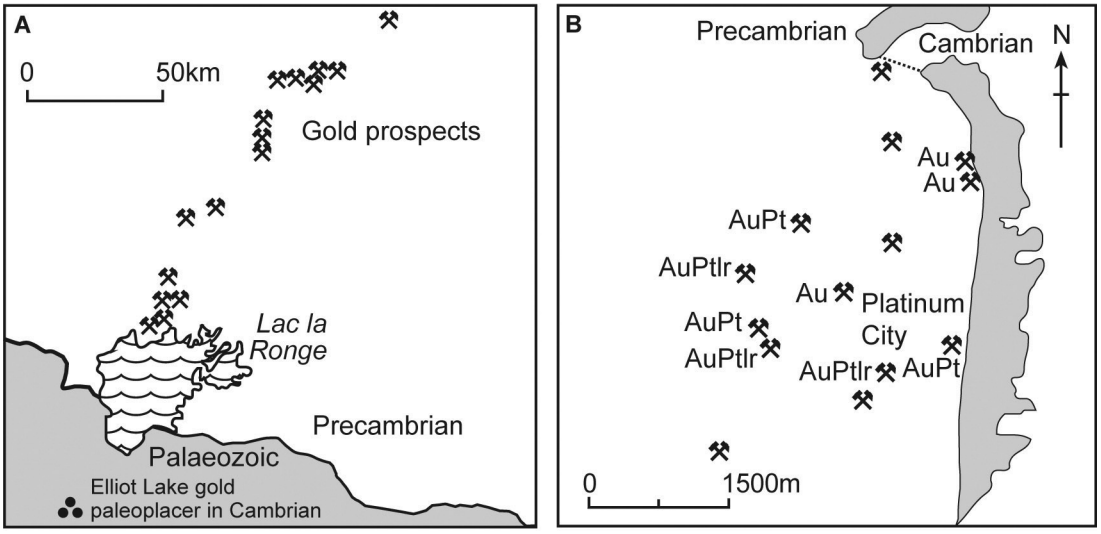

Fig. 3. Maps of gold prospects in Precambrian rocks passing below sub-Cambrian unconformity. (A) Lac la Ronge district, Saskatchewan, where gold paleoplacer also occurs in Cambrian (after Rogers, 2011); (B) Platinum City district, Wyoming, where gold occurs with platinum and iridium ores (after Hausel, 1989).

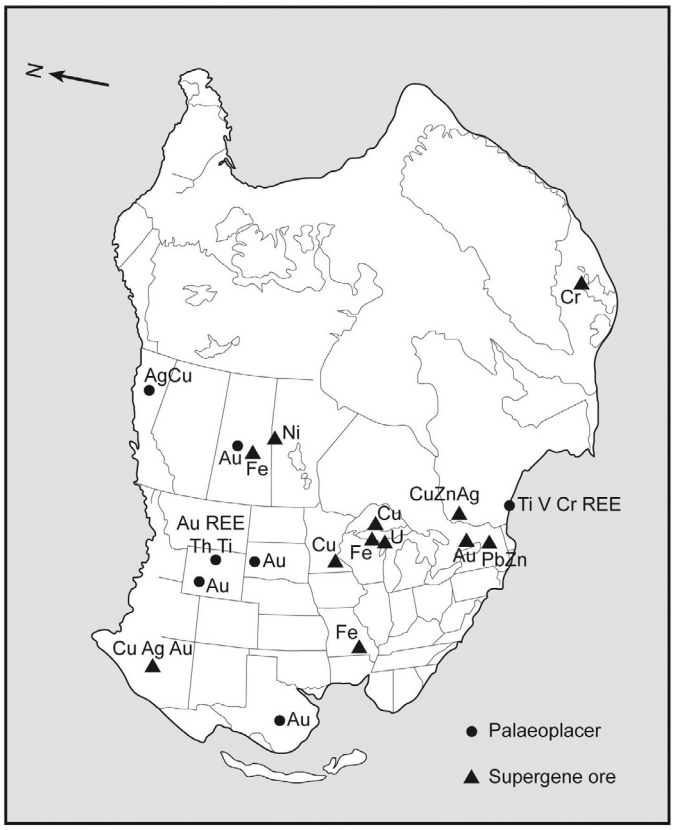

Fig. 4. Detailed reconstruction for Laurentia (Colorado Plateau Geosystems, 2011) showing location of supergene ores and palaeoplacers on the sub-Cambrian surface (data sources in text).

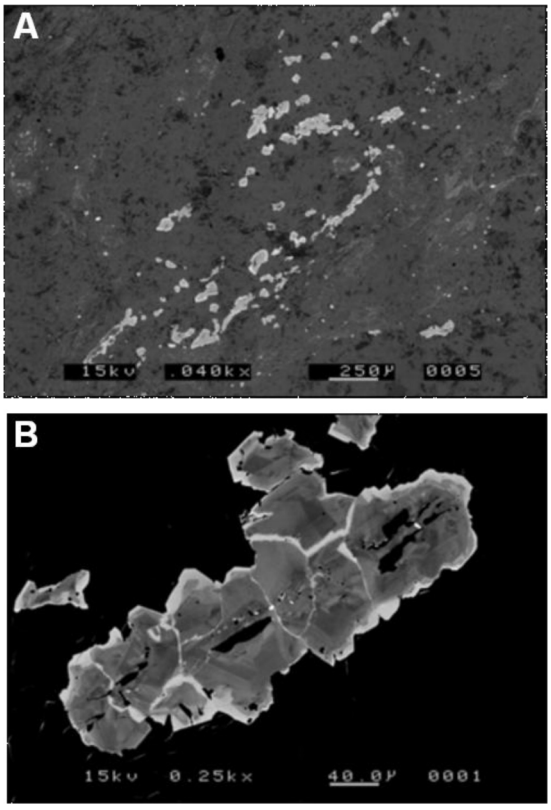

Fig. 5. Backscattered electron image of (A) multiple grains of Cr-rich phosphosulphate (bright) within pinite groundmass; (B) zoned REE-Sr phosphate (bright) within pinite groundmass, sub-Cambrian surface, northern Scotland.

The Archean gneiss includes basic layers rich in chromium (O'Hara, 1961). The bulk chromium content of unaltered gneisses in the region is 320 ppm (Weaver and Tarney, 1981). The pinite is locally the chromium-rich mica fuchsite, which allows us to take advantage of the fact that chromium is emerging as a sensitive tracer of continental weathering (Frei et al., 2009; Frei and Polat, 2013; Berger and Frei, 2013; Crowe et al., 2013; Konhauser et al., 2011). The pinite includes numerous authigenic mineral phases that are suspended within it, particularly minerals enriched in chromium. They include a range of phosphate and phosphosulphate minerals, in which strontium is a major cation (e.g., up to 10 wt.% SrO). REE are also enriched (Fig. 5). These minerals are zoned and with well-developed crystal faces (Fig. 5), so are clearly authigenic rather than detrital. Denudation of the weathered surface is also evident as clasts of clay-altered feldspar, haematized quartz and the angular nature of quartz clasts in the lowermost Cambrian deposits.

Widespread planation of the deeply weathered, metal-enriched Precambrian–Cambrian surface delivered a quantity of metalliferous detritus and solute into the ocean which far exceeded normal element fluxes throughout geological history. To assess if enrichment coincided with the basal Cambrian geochemical anomaly, high-precision age constraints for the planation are required. Dating of planation, essentially hiatuses in terrestrial sedimentation, is problematic. However, in several parts of the world, including Scotland (Allison et al., 1992), Pennsylvania (Simpson et al., 2002) and Korea (Kim and Lee, 2003), the clay alteration products on the sub-Cambrian surface contain abundant pinite, suggesting a global weathering event. The pinite is potassium-rich and therefore theoretically amenable to $^{40}Ar/^{39}Ar$ dating.

3. Analytical methods

3.1. $^{40}Ar/^{39}Ar$ geochronology

We have dated the mica (pinite) from two localities in weathered Archean gneiss near Durness, Scotland using the $^{40}Ar/^{39}Ar$ CO_2 laser step-heating approach. The samples are from Rispond (National Grid Reference NC 432621) and Ceannabeinne (NC 437662). The samples contained mica crystals of between 100 and 125 μm in dimension and hence were deemed suitable for $^{40}Ar/^{39}Ar$ dating without the risk of inducing ^{39}Ar and ^{37}Ar recoil (VanLaningham and Mark, 2011). The samples were crushed gently in mortar and pestle and sieved. The 100–125 μm fraction was washed in distilled water and subsequently methanol. The pinite (amorphous K-mica) has a distinctive green colour and pristine (unaltered) fragments were handpicked under binocular microscope for $^{40}Ar/^{39}Ar$ dating.

Samples were loaded into high-purity Al discs for irradiation. International standards GA1550 biotite (98.79 ± 0.96), a primary standard against which the Fish Canyon sanidine age (FCs) (28.02 ± 0.16 Ma) of Renne et al. (1998) was calibrated, was loaded adjacent to the pinite samples of unknown age. Crystals of MMhb-1 hornblende (523.1 ± 4.6 Ma; Renne et al., 1998) and FCs were also loaded adjacent to the pinite samples to check J-parameter accuracy. Samples were irradiated for 40 h in the Cd-lined RODEO facility of the McMaster reactor. GA1550 (n = 50) and FCs (n = 15) were analyzed by total fusion with a focused CO_2 laser. MMhb-1 hornblende was step-heated by CO_2 laser. Using J-parameter measurements from GA1550, both FCs and MMhb-1 yield ages that overlap with those defined by Renne et al. (1998), indicating appropriate measurements of the J-parameter from GA1550 for the determination of unknown ages.

Single grains of pinite were loaded into a Cu planchette in an ultra-high vacuum laser cell with a doubly pumped ZnSe window. Using a CO_2 laser, the pinite crystals were step-heated. All gas fractions were subjected to 180 s of purification with two SAES GP50 getters (one at room temperature the other at 450 °C) and a cold finger maintained at −95.5 °C using a mixture of dry ice ($CO_{2[s]}$) and acetone. Argon isotope ratios (i.e., ion beam intensities) were measured using a GV Instruments ARGUS V multi-collector noble gas mass spectrometer (e.g., Mark et al., 2009, 2011a). The mass spectrometer has a measured sensitivity of 7×10^{-14} moles/volt. Both the extraction and cleanup processes were automated, as was the mass data acquisition. Backgrounds were measured after every two analyses of unknowns. Average backgrounds ± standard deviation ($n = 41$: ^{40}Ar 1.01×10^{-15} moles, ^{39}Ar 3.03×10^{-17} moles, ^{38}Ar 1.50×10^{-17} moles, ^{37}Ar 7.11×10^{-17} moles, ^{36}Ar 1.01×10^{-17} moles) from the entire run sequence were used to correct raw isotope measurements of unknowns. Mass discrimination was monitored by analysis of air pipettes after every four analyses ($n = 23$, $^{40}Ar/^{36}Ar = 300.5 \pm 0.2$). The Ar isotope data were corrected for backgrounds, mass discrimination, and reactor-produced nuclides and processed using standard data reduction protocols. The decay constants of Steiger and Jäger (1977) and atmospheric argon ratios of Lee et al. (2006), the latter independently verified by Mark et al. (2011b), were employed.

The BGC software *MassSpec* was used for data regression. Data are displayed on ideograms and isotope correlation plots (inverse isochron plots). Data are reported according to the recommendations of Renne et al. (2009).

3.2. Cr isotope analysis

A sample powder aliquot (amount adjusted to yield ~2 μg Cr in the final separate) was spiked with an adequate amount (corresponding to ~700 ng of Cr) of a ^{50}Cr–^{54}Cr double spike and digested in a HF:HNO_3 mixture in a closed PFA vial on a hot plate at 150 °C. After heating to dryness, the sample was taken up in aqua regia and reheated to 170 °C for 2 h to destroy any fluoride complexes that may have formed during the digestion, and to ensure spike-sample homogenization. After renewed drying, the sample was then taken up in 6 M hydrochloric acid and passed over an anion column charged with ~2 ml of AG-1X12 200-400 mesh resin to remove Fe. Then the sample was processed over another cation exchange column charged with 2 ml AG-1X12 200-400 mesh resin in 0.5 M hydrochloric acid, and a pure Cr separate was collected after a modified elution procedure described by Trinquier et al. (2008). The procedure yield for Cr in this separation method is about 60–70%, and Cr procedure blanks were in the order of 2–4 ng, which is negligible compared to the amount of chromium separated from the sample studied.

The addition of a ^{50}Cr–^{54}Cr double spike of known isotope composition to the sample before chemical purification allowed accurate correction of both the chemical and the instrumental shifts in Cr isotope abundances (Ellis et al., 2002; Schoenberg et al., 2008). With this method, we achieve a 2 sigma external reproducibility of the δ^{53}Cr value with 1.0 μg Cr loads of the NIST SRM 979 standard on our IsotopX/GV IsoProbe T thermal ionization mass spectrometer (TIMS) of ±0.05‰ with ^{52}Cr signal intensities of 1 V and of ±0.08‰ for ^{52}Cr beam intensities of 500 mV, with δ^{53}Cr at −0.07‰. Since the double spike correction references Cr isotope compositions of samples as the per mil difference to the isotope composition of the NIST SRM 3112a Cr standard (which was used for the spike calibration (Schoenberg et al., 2008), to maintain inter-laboratory comparability of Cr isotope data, we recalculated our data of natural samples relative to the certified Cr isotope standard NIST SRM 979 as follows:

$$\delta^{53}\text{Cr sample (SRM 979)} = [^{53}\text{Cr}/^{52}\text{Cr sample}/^{53}\text{Cr}/^{52}\text{Cr SRM 979}) - 1] \times 1000 \quad (1)$$

Cr isotope measurements were performed on an IsotopX/GV IsoProbe T TIMS equipped with eight Faraday collectors that allow simultaneous collection of all four chromium beams (^{50}Cr+, ^{52}Cr+, ^{53}Cr+, ^{54}Cr+) together with ^{49}Ti+, ^{51}V+, and ^{56}Fe+ as monitors for small interferences of these masses on ^{50}Cr and ^{54}Cr. Cr separates were measured from Re filaments at 1000–1100 °C and loaded with ultraclean water into a mixture of 3 μl silica gel, 0.5 μl 0.5 M H_3BO_3 and 0.5 μl 0.5 M H_3PO_4.

The δ^{53}Cr value of a sample was calculated as the average of four repeated analyses. We spiked our sample with an aliquot of the double spike used by (Schoenberg et al., 2008) in their study of silicates and oxides of magmatic and metamorphic rocks, and employed the double spike correction developed by their group.

3.3. Sr isotope analysis

Samples for $^{87}Sr/^{86}Sr$ analysis were leached in 2.5 ml 0.15 M ammonium acetate (NH_4OAc) for 2 h prior to dissolution of calcite in 1 M acetic acid (HOAc) for a further 2 h at room temperature (see Gorokhov et al., 1995; Kuznetsov et al., 1997; Shields, 1999; Bailey et al., 2000). The pre-dissolution leach in NH_4OAc was used to remove non-stoichiometric Sr (Walls et al., 1977; Gao, 1990), which has been shown to be significantly more radiogenic than Sr bound in lattice sites and sufficiently abundant to contaminate the pinite $^{87}Sr/^{86}Sr$ signature (e.g., Gorokhov et al., 1995; Kuznetsov et al., 1997; Thomas, 1999; Bailey et al., 2000). Strontium was separated from the supernatant by standard ion-exchange techniques using resin columns and $^{87}Sr/^{86}Sr$ analyzed by thermal ionization mass spectrometry on a VG 54E single collector or a VG Sector 54-30 multiple-collector mass spectrometer. The $^{87}Sr/^{86}Sr$ ratio was corrected for mass fractionation using $^{86}Sr/^{88}Sr = 0.1194$ and an exponential law. Precision on the VG 54E was better than ±0.00004 (2 SE) and repeat analysis of NBS 987 gave $^{87}Sr/^{86}Sr = 0.71024 \pm 3$ (1 SD, $n = 20$). On the VG Sector 54-30, precision was better than ±0.00002 (2 SE) and repeat analysis of NBS 987 gave $^{87}Sr/^{86}Sr = 0.710243 \pm 0.000010$ (1 SD, $n = 88$). Data reported are time correct for Rb decay (reported as $^{87}Sr/^{86}Sr_t$).

4. Results

4.1. $^{40}Ar/^{39}Ar$ geochronology

Two aliquots of both samples (Rispond and Ceannabeinee) were analyzed. Fig. 6 shows the data. All four aliquots yielded 100% ^{39}Ar plateaus with ages that are indistinguishable at the 1 sigma (68%) confidence level (analytical precision). Data cast on an isotope correlation plot define a binary mixing line with initial trapped components indistinguishable from modern day atmospheric $^{40}Ar/^{36}Ar$, and a K-correlated radiogenic component yields an age indistinguishable from the plateau ages. Fig. 6 shows the weighted average of the four plateau ages. Relative to the GA1550 at 98.79 Ma (Renne et al., 1998) and the decay constants of Steiger and Jäger (1977), the samples define a robust and statistically sound age for the pinite of: 537.85 ± 0.18 Ma (1 sigma, analytical precision only).

The $^{40}Ar/^{39}Ar$ method is a relative dating technique with all ages referenced back to a standard of known age. Recently Renne et al. (2010, 2011) published an optimization model that used constraints from ^{40}K activity, K–Ar isotopic data, and pairs of ^{238}U–^{206}Pb and $^{40}Ar/^{39}Ar$ data as inputs for estimating the partial

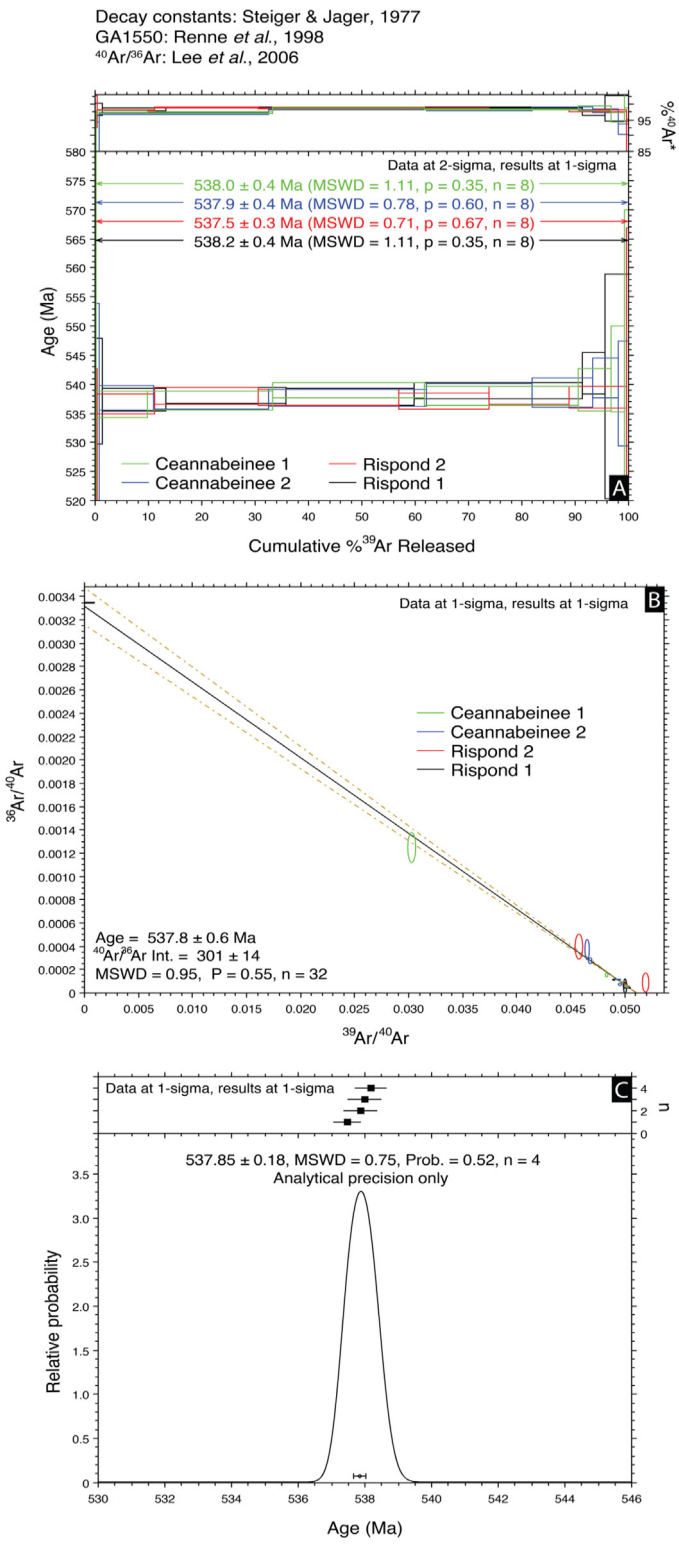

Fig. 6. (a) Step-heating spectra for all four sample analyses. All samples define 100% ^{39}Ar plateaux (b) isotope correlation plot showing inverse isochron for all step-heating data. Data define an age within uncertainty of the step-heating spectra and a trapped component (albeit at low precision) that is indistinguishable from air. There is no evidence for irradiation-induced recoil of ^{37}Ar or ^{39}Ar. (c) Weighted average of all four plateau ages.

decay constants of ^{40}K and ^{40}Ar*/^{40}K ratio of FCs. This calibration has reduced systematic uncertainties (i.e., accuracy) in the ^{40}Ar/^{39}Ar system from c. 2.5% to less than 0.25%. The optimization model has also yielded an age for FCs that overlaps at the 2 sigma confidence level with the astronomically tuned FCs age of Kuiper et al. (2008), but beyond the 2 sigma confidence level of Rivera et al. (2011). New ^{40}Ar/^{39}Ar data (Renne et al., 2013) for the Cretaceous-Palaeogene (K-Pg) boundary show that the calibration of Rivera et al. (2011) places the K-Pg boundary exactly intermediate between two possible choices of 405 ka orbital eccentricity cycles. The implication is that the astronomically tuned age for FCs (Rivera et al., 2011) is inconsistent with any astronomically tuned age for the K-Pg boundary. It is the ^{40}Ar/^{39}Ar calibration of Renne et al. (2011) that is proven to be the most accurate with the astronomically tuned age (Kuiper et al., 2008) for the K-Pg boundary (Renne et al., 2013).

Therefore, to present the most accurate ^{40}Ar/^{39}Ar age for the pinite we have recalculated our age (537.85 ± 0.18 Ma) relative to the optimization model of Renne et al. (2010, 2011) using the approach of Ellis et al. (2012) and Mark et al. (in press). All calculations were performed using the calculations outlined by Renne et al. (2010) and using the optimization model spreadsheet available directly from Prof. Paul Renne at the Berkeley Geochronology Centre. Our data define an age of 542.62 ± 0.38 Ma (1 sigma, Renne et al., 2011, full external precision). The age and its 0.07% 1 sigma uncertainty includes all sources of error, including decay constant uncertainty, and is hence directly comparable to all timescales as defined by other chronometers (e.g., U-Pb chronologies). This age is discussed throughout as the most accurate pinite ^{40}Ar/^{39}Ar age.

4.2. Cr and ^{87}Sr/^{86}Sr isotope analysis

A δ^{53}Cr value of −1.32 ± 0.08‰ was obtained for a Cr-rich (7498 ppm) sample of the pinite from Rispond. A ^{87}Sr/^{86}Sr$_t$ ratio of 0.75602 ± 0.00002 was obtained for the same sample of pinite.

5. Discussion

It is conceivable that pinite could be formed during a metamorphic event or by alteration of metamorphic/plutonic rocks (e.g., Marchand et al., 1982; Farina et al., 2012). However, we can be confident that in this case the pinite is related to the surface weathering environment, because:

(i) The 542 Ma date does not coincide with any orogenic/metamorphic event in the region, and the history of the crust in this region is known in detail.
(ii) Known subsequent events of fluid flow related to orogenesis in the region, including the Grampian and Scandian phases of the Caledonian Orogeny (Mark et al., 2007), are not recorded in the pinite, and so have not overprinted it.
(iii) An earlier weathering surface between Neoproterozoic sedimentary rocks (Torridon Group) and Lewisian in the same region, which also contains clay minerals, has not been converted to pinite, and does not yield the 542 Ma date (authors' unpublished data).
(iv) The basal conglomerate of the overlying Cambrian contains clasts of pinite-bearing material.
(v) The pinite extends downwards from the unconformity along zones of easier penetration, such as pegmatite veins, consistent with selective weathering.
(vi) The pinitized rocks also contain haematite, indicating an oxidized environment.
(vii) The comparable occurrences of pinite on the sub-Cambrian surface in the USA and Korea indicate a distinctive degree of weathering on this surface.

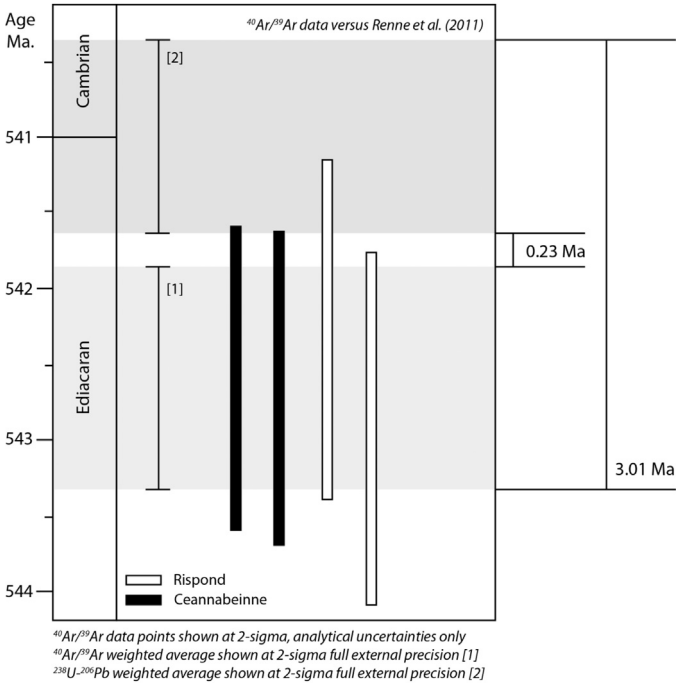

Fig. 7. $^{40}Ar/^{39}Ar$ data for the four individual samples (shown at 2 sigma uncertainty) plotted against the Precambrian–Cambrian boundary age as defined by the latest Geological Time Scale (GTS2012) (Gradstein et al., 2012). Weighted average [1] $^{40}Ar/^{39}Ar$: 542.62 ± 0.76 Ma (Renne et al., 2011), weighted average [2] ^{238}U–^{206}Pb: 541.00 ± 0.63 Ma (Bowring et al., 2007). Both weighted averages are shown at 2 sigma uncertainty and as grey bands in the figure. The figure shows that there is at a minimum 0.23 Ma between the age of the Precambrian–Cambrian boundary and the age of the pinite and at a maximum (allowing for uncertainties in the dating techniques) there is a window of 3.01 Ma.

The sub-Cambrian basement surface in Scotland is Archean with mid-Proterozoic pegmatites, so in theory the clay weathering surface could have formed at any stage in a time interval of over a billion years. The 542.62 ± 0.38 Ma age of the clay alteration (pinite) is just beyond the 2 sigma uncertainty interval of the Precambrian–Cambrian boundary (Fig. 7), which has a ^{238}U–^{206}Pb of 541.00 ± 0.63 Ma (2 sigma, full external uncertainty; Bowring et al., 2007; Gradstein et al., 2012). Allowing for the associated 2 sigma age uncertainties (full external precision), there is a minimum of 0.23 Ma and a maximum of 3.01 Ma temporally separating the formation of the pinite and the Precambrian–Cambrian boundary. The peneplanation that flushed the metals to the ocean geologically immediately preceded the boundary. Thus, the alteration occurred very shortly before the Cambrian transgression. This is consistent with other evidence for weathering immediately before the Cambrian transgression: Provenance data for the Cambrian sandstones in North Africa indicate a predominantly late Neoproterozoic source (detrital zircon) (Avigad et al., 2003, 2005; Morag et al., 2011), the clay-weathered surface in England (Avalonia) lies on late Neoproterozoic volcanic rocks (McIlroy et al., 1998), a regional unconformity in Siberia is underlain by karstified late Neoproterozoic limestones (Pelechaty et al., 1996) and the hiatus in Australia, Canada, England and elsewhere resides above rocks containing Ediacaran (late Neoproterozoic) fossils (Cowie and Brasier, 1989). Furthermore, the peneplain is parallel to the overlying transgressive deposits, indicating a contiguous period of erosion and sedimentation. The exceptional global distribution and intensity of this event, proximal to the Precambrian–Cambrian boundary, suggests that scrutiny of the terrestrial surface may help us understand the changes in biogeochemistry recorded in the marine sections across the Precambrian–Cambrian boundary.

A $\delta^{53}Cr$ value of −1.32 ± 0.08‰ for the pinite is distinctly different from values of +0.2 to +4.9‰ measured on late Ediacaran Fe-rich cherts and banded iron formation from Uruguay which were explained by isotopically heavy Cr(VI) influx to the basin after pulses of oxidative weathering on land and Fe(II) accumulation in the water column (Frei et al., 2009). The strongly negatively fractionated $\delta^{53}Cr$ value of the pinite is consistent with a concentration of chromium by oxidative terrestrial weathering, in which the light isotope is preferentially retained in the weathering soils (Crowe et al., 2011, 2013; Frei and Polat, 2013; Berger and Frei, 2013).

The $^{87}Sr/^{86}Sr_t$ ratio of 0.75602 ± 0.00002 of the pinite is much more radiogenic than the contemporary and Late Neoproterozoic-Cambrian seawater $^{87}Sr/^{86}Sr_t$ composition of ~0.707–0.709 (Shields, 2007), and confirms that strontium enrichment on the Scottish sub-Cambrian surface was predominantly due to in situ weathering of continental crustal rocks rather than precipitation from sea water. In summary, the isotopic data from Scotland indicate an enrichment of metals (and other elements) by terrestrial weathering, characteristic of the worldwide concentration of metals at the Precambrian–Cambrian boundary.

As the widespread planar unconformity sites are parallel with overlying Cambrian sandstone beds, the redistribution of metals was an integral aspect of the Cambrian transgression. The petrography of the metalliferous concentration horizon from Scotland allows us to ground-truth what was being delivered to the ocean by erosion. It includes numerous authigenic mineral phases, including the chromium mica fuchsite, a range of strontium-rich phosphosulphate minerals, and rare earth phosphates. The occurrences of mineral phases in the weathering profile in Scotland enriched in chromium, REE, phosphorus, and strontium, implies a very strong relationship with an early Cambrian ocean enriched in metals, REE, phosphorus, and radiogenic strontium.

Globally, where the sub-Cambrian surface is well-preserved, it is altered to a depth of 10 m or more and >100 m in some ore deposits (e.g., James et al., 1968; Di Prisco and Springer, 1991; May and Dinkowitz, 1996; Avigad et al., 2005). Clasts of clay-weathered rock in the basal pebbly layers of the Cambrian sandstones (Avigad et al., 2003, 2005; Di Prisco and Springer, 1991) show that the sub-Cambrian surface was substantially denuded of its altered cover during the transgression, and most supergene deposits were probably eroded away into the early Cambrian oceans. These observations imply that an average of at least 1 m of alteration products was denuded. On the (current) northern margin of the Pan-African Orogen, the transgression can be traced for 6000 km by 1500 km (Avigad et al., 2005). The transgression of North America covered a comparable area, and assuming a conservative similar area for the rest of the world, denudation of 1 m over this area would yield about 7.6×10^{16} kg rock. If this rock contained just the crustal mean values of metals (i.e., without enrichment), it would represent a quantity of chromium 30 times, iron and REE each 10^2 times, iridium 5 times and gold 10^{-2} times the current content dissolved in the world's oceans. If the quartz sandstones of the Cambrian transgression were derived largely from the sub-Cambrian weathering mantle (Peters and Gaines, 2012; Avigad et al., 2005), their typical thickness of hundreds of metres implies a much greater denudation than the mean 1 m assumed. A mean erosion of 10 m and a tenfold supergene enrichment would cause a flux of almost all metals in excess of the volume in the current ocean.

6. Conclusions

The sub-Cambrian surface penetrated numerous Precambrian-hosted ore deposits, many of which were conspicuously altered before subsequent reburial by Cambrian and younger rocks. Alteration included the concentration of metals by supergene

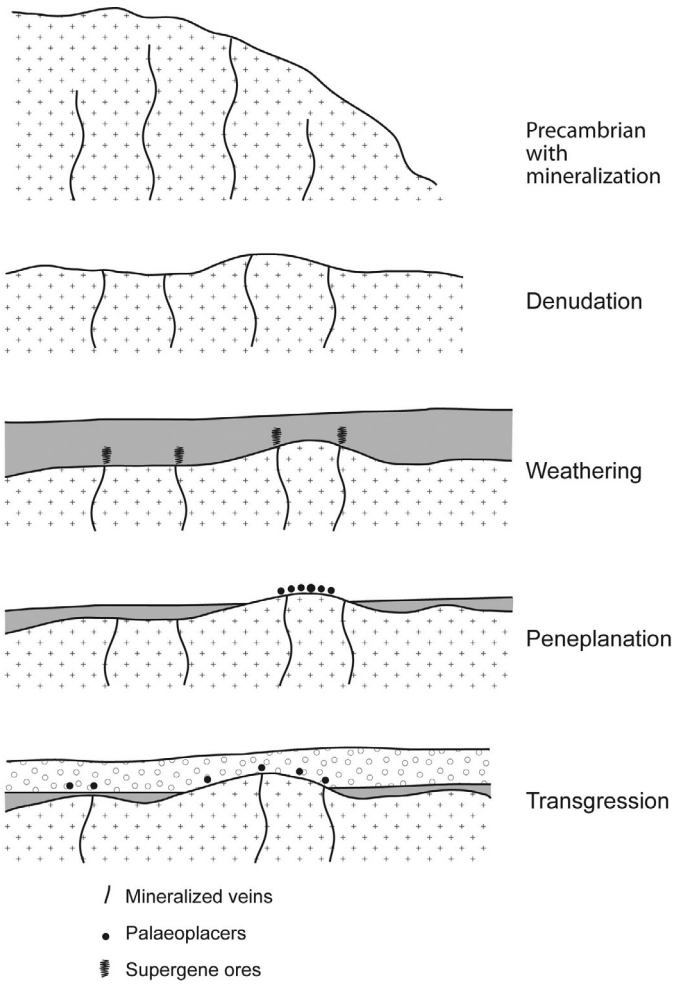

Fig. 8. Schematic evolution of sub-Cambrian surface with exposed Precambrian ores, weathered supergene ores and palaeoplacers, followed by Cambrian transgression.

enrichment and by the formation of metalliferous palaeoplacers on the sub-Cambrian surface (Fig. 8). This exceptional concentration of metal was then available for delivery to the early Cambrian ocean, facilitated by the global Cambrian transgression and accompanying planation. The early Cambrian ocean is known to have been anomalously metalliferous, implying that such a delivery of metals did occur. This unprecedented delivery of metals thereby must have contributed to the exceptional geochemical environment that hosted the rapid diversification of life in the early Cambrian ocean (Maloof et al., 2010; Peters and Gaines, 2012).

Investigation of chromium-rich clay alteration products on the sub-Cambrian surface in Scotland shows:

(i) Enrichment of elements, including heavy metal, rare earth elements, strontium and phosphorus occurred on the surface, which strongly matches enrichments recorded in the early Cambrian ocean.
(ii) The clay alteration dates to just before the Precambrian–Cambrian boundary, indicating that this boundary defined by the fossil record coincides with a marked environmental event which witnessed intense chemical weathering.
(iii) The alteration was due to terrestrial weathering, rather than precipitation of minerals from seawater.
(iv) Planation postdated the alteration of the sub-Cambrian surface, and would have delivered the concentrated metals and other elements to the transgressing Cambrian ocean. The Cambrian seawater is predictably characterized by positively fractionated $\delta^{53}Cr$ values, as a consequence of oxidative removal from the landmasses and transport to the oceans of heavy Cr(VI).

Acknowledgments

Financial support through the Danish Agency for Science, Technology and Innovation grant nr. 11-103378 to RF and through the Danish National Research Foundation's Center of Excellence Nord-CEE (DNRF grant number DNRF53) is highly appreciated.

The Natural Environment Research Council is thanked for continued funding of the Argon Isotope Facility at the Scottish Universities Environmental Research Centre. Ross Dymock and Jim Imlach (SUERC) are thanked for sample preparation and technical assistance. Martin Brasier (University of Oxford) is thanked for useful discussion.

References

Al-Hwaiti, M., Zoheir, B., Lehmann, B., Rabba, I., 2010. Epithermal gold mineralization at Wadi Abu Khushayba, southwestern Jordan. Ore Geol. Rev. 38, 101–112.
Allison, I., Cardenas, F.A., Kronberg, B.I., 1992. Precambrian muscovite-quartz (agalmatolite) paleosols from Scotland and Canada. Can. J. Earth Sci. 29, 2523–2529.
Alvaro, J.J., Subias, I., 2011. Interplay of phosphogenesis and hydrothermalism in the latest Ediacaran rift of the High Atlas, Morocco. J. Afr. Earth Sci. 59, 51–60.
Ambrose, J.W., 1964. Exhumed paleoplains of the Precambrian Shield of North America. Am. J. Sci. 262, 817–857.
Amthor, J.E., Gtotzinger, J.P., Schroder, S., Bowring, S.A., Ramezani, J., Martin, M.W., Matter, A., 2003. Extinction of *Cloudina* and *Namacalathus* at the Precambrian–Cambrian boundary in Oman. Geology 31, 431–434.
Asael, D., Matthews, A., Bar-Matthews, M., Halicz, L., 2007. Copper isotope fractionation in sedimentary copper mineralization (Timna Valley, Israel). Chem. Geol. 243, 238–254.
Avigad, D., Kolodner, K., McWilliams, M., Persing, H.M., Weissbrod, T., 2003. Origin of northern Gondwana Cambrian sandstone as revealed by SHRIMP dating of detrital zircons. Geology 31, 227–230.
Avigad, D., Sandler, A., Kolodner, K., Stern, R.J., McWilliams, M., Miller, N., Beyth, M., 2005. Mass-production of Cambro-Ordovician quartz-rich sandstones as a consequence of chemical weathering of Pan-African terranes: environmental implications. Earth Planet. Sci. Lett. 240, 818–826.
Awmack, H.J., 1994. Exploration Program Tuchodi Proterozoic Basin. British Columbia Ministry of Energy, Mines and Petroleum Resources Assessment Report 24., pp. 603.
Bailey, T.R., McArthur, J.M., Prince, H., Thirlwall, M.F., 2000. Dissolution methods for strontium isotope stratigraphy: whole rock analysis. Chem. Geol. 167, 313–319.
Baldwin, A.B., Gross, W.H., 1967. Possible explanations for the localization of residual hematite ore on a Precambrian iron formation. Econ. Geol. 62, 95–108.
Bayley, R.W., Proctor, P.D., Condie, K.C., 1973. Geology of the South Pass Area, Fremont County, Wyoming. U.S. Geological Survey Professional Paper 793.
Berger, A., Frei, R., 2013. The fate of chromium during tropical weathering: a laterite profile from Central Madagascar. Geoderma 213, 521–532.
Bjørlykke, A., Cumming, G.L., Krstic, D., 1990. New isotopic data from davidites and sulfides in the Bidjovagge gold-copper deposit, Finnmark, northern Norway. Miner. Petrol. 43, 1–21.
Blanco, G., Zimmermann, U., Germs, G.J.B., Gaucher, C., 2006. Provenance study on 'Black Sands': a case study from the Lower Cambrian Fish River sub-group (Nama Group, Namibia). In: V South American Symposium on Isotope Geology (Proceedings IGCP 478), pp. 204–205.
Bornhorst, T.J., 2002. Precambrian supergene alteration of native copper deposits in the Keweenaw Peninsula, Michigan. In: Geological Society of America Annual Meeting abstracts No. 163-5.
Bowring, S.A., Grotzinger, J.P., Condon, D.J., Ramezani, J., Newall, M.J., Allen, P.A., 2007. Geochronologic constraints on the chronostratigraphic framework of the Neoproterozoic Huqf supergroup, Sultanate of Oman. Am. J. Sci. 307, 1097–1145.
Brown, J.S., 1936. Supergene sphalerite, galena and wilmenite at Balmat, N.Y. Econ. Geol. 31, 331–354.
Cheesman, R.L., 1964. The geology of the Choiceland iron deposit, Saskatchewan. Can. Min. Metall. Bull. 57, 715–718.
Colorado Plateau Geosystems, Inc., 2011. Library of Paleogeographic Maps of Ron Blakey, http://cpgeosystems.com/paleomaps.html
Cook, P.J., 1992. Phosphogenesis around the Precambrian-Phanerozoic transition. J. Geol. Soc., Lond. 149, 615–620.
Cowie, J.W., Brasier, M.D. (Eds.), 1989. The Precambrian–Cambrian Boundary. Clarendon Press, Oxford.
Crowe, S.A., Dössing, L.N., Maclean, L.C.W., Frei, R., Fowle, D.A., Mussi, A., Canfield, D.E., 2011. Oxidative weathering fractionates chromium isotopes. Mineral. Mag. 75, 706.

Crowe, S.A., Døssing, L.N., Beukes, N.J., Bau, M., Kruger, S.J., Frei, R., Canfield, D.E., 2013. Atmospheric oxygenation three billion years ago. Nature 501, 535–539.

Cumming, G.L., Krstic, D., 1991. Geochronology at the Namew Lake Ni–Cu deposit, Flin Flon area, Manitoba, Canada: a Pb/Pb study of whole rocks and ore minerals. Can. J. Earth Sci. 28, 1328–1339.

Di Prisco, G., Springer, J.S., 1991. The Precambrian-Paleozoic unconformity and related mineralization in southeastern Ontario. Ontario Geological Survey Report 5751.

Duffin, M.E., 1989. Nature and origin of authigenic K-feldspar in Precambrian basement rocks of the North American midcontinent. Geology 17, 765–768.

Dutton, C.E., Zimmer, P.W., 1968. Iron ore deposits of the Menominee district, Michigan. In: Ridge, J.D. (Ed.), Ore Deposits of the United States, 1933–1967. The American Institute of Mining, Metallurgical, and Petroleum Engineers, Inc., New York, pp. 539–549.

Ellis, A.S., Johnson, T.M., Bullen, T.D., 2002. Chromium isotopes and the fate of hexavalent chromium in the environment. Science 295, 2060–2062.

Ellis, B.S., Mark, D.F., Ptitchard, C.J., Wolff, J.A., 2012. Temporal dissection of the Huckleberry Ridge Tuff using the $^{40}Ar/^{39}Ar$ dating technique. Quaternary Geochronol. 9, 34–41.

Emery, J.A., 1968. Geology of the Pea Ridge Iron ore body, in RIDGE. In: John, D. (Ed.), Ore Deposits of the United States, 1933–1967. The American Institute of Mining, Metallurgical, and Petroleum Engineers, Inc., New York, pp. 360–369.

Farina, F., Stevens, G., Villaros, A., 2012. Multi-batch, incremental assembly of a dynamic magma chamber: the case of the Peninsula pluton granite (Cape Granite Suite, South Africa). Mineral. Petrol. 106, 193–216.

Ferguson, L.K., Fallick, A.E., Allison, I., 1998. Tourmaline in a sub-Cambrian palaeosol on the Proterozoic Lewisian rocks of NW Scotland. J. Geol. Soc., Lond. 155, 725–731.

Förster, H., Jafarzadeh, A., 1994. The Bafq mining district in central Iran – a highly mineralized Infracambrian volcanic field. Econ. Geol. 89, 1697–1721.

Frei, R., Polat, A., 2013. Chromium isotope fractionation during oxidative weathering – implications from the study of a Paleoproterozoic (ca. 1.9 Ga) paleosol, Schreiber Beach, Ontario, Canada. Precambrian Res. 224, 434–453.

Frei, R., Guacher, C., Poulton, S.W., Canfield, D.E., 2009. Fluctuations in Precambrian atmospheric oxygenation recorded by chromium isotopes. Nature 461, 250–253.

Gao, G., 1990. Geochemical and isotopic constraints on the diagenetic history of a massive stratal, late Cambrian (Royer) dolomite, Lower Arbuckle Group, Slick Hills, SW Oaklahoma, USA. Geochim. Cosmochim. Acta 54, 1979–1989.

Gauthier, M., Chartrand, F., Trottier, J., 1994. Metallogenic epochs and metallogenic provinces of the Estrie-Beauce Region, southern Quebec Appalcahians. Econ. Geol. 89, 1322–1360.

Gorokhov, I.M., Semikhatov, M.A., Baskavov, A.V., Kutyavin, E.P., Mel'nikov, N.N., Sochava, A.V., Turchenko, T.L., 1995. Sr isotopic composition in Riphean, Vendian, and Lower Cambrian carbonates from Siberia. Stratigr. Geol. Correl. 3, 1–28.

Gradstein, F.M., Og, J.G., Schmitz, M.D., Ogg, J.M., 2012. The Geological Time Scale 2012. Elsevier, Amsterdam.

Hausel, W.D., 1989. The geology of Wyoming's precious metal lode and placer deposits. Geol. Surv. Wyo. Bull. 68, 248.

Hausel, W.D., Graves, W.H., 1996. Placers and paleoplacers of the Bighorn Basin. Wyo. Geol. Assoc. Guidebook 47, 273–280.

Heylmun, E.B., 2001. Gold in Texas. Prospect. Mining J. 71 (2), 28–30.

Jackson, E.D., 1968. The chromite deposits of the Stillwater Complex, Montana. In: Ridge, J.D. (Ed.), Ore Deposits of the United States, 1933–1967. The American Institute of Mining, Metallurgical, and Petroleum Engineers, Inc., New York, pp. 1496–1510.

James, H.L., Dutton, C.E., Pettijohn, F.J., Wier, K.L., 1968. Geology and Ore Deposits of the Iron River-Crystal Falls District, Iron County, Michigan. U.S. Geological Survey Professional Paper 570.

Johnstone, G.S., Mykura, W., 1989. British Regional Geology. The Northern Highlands of Scotland, Fourth Edition. Her Majesty's Stationery Office, London.

Kim, Y., Lee, Y.I., 2003. A new Late Proterozoic stratum in South Korea. Geosci. J. 7, 47–52.

Kim, Y., Lee, Y.I., 2006. Early evolution of the Duwibong Unit of the Lower Paleozoic Joseon Supergroup, Korea: a new view. Geosci. J. 10, 391–402.

Konhauser, K.O., Lalonde, S.V., Planavsky, N.J., Pecoits, E., Lyons, T.W., Mojzsis, S.J., Rouxel, O.J., Barley, M.E., Rosière, C., Fralick, P.W., Kump, L.R., Bekker, A., 2011. Aerobic bacterial pyrite oxidation and acid rock drainage during the Great Oxidation Event. Nature 478, 369–373.

Konstantinovskii, A.A., 2001. Potential mineral resources of the Anabar Anteclise cover. Lithol. Min. Resour. 36, 406–418.

Krendelev, F.P., 1966. Prospects of exploration for ancient metalliferous conglomerates in Siberia. Int. Geol. Rev. 8, 716–730.

Kuiper, K.F., Deino, A., Hilgen, F.J., Krijgsman, W., Renne, P.R., Wijbrans, J.R., 2008. Synchronizing the rock clocks of Earth History. Science 320, 500–504.

Kuznetsov, A.B., Gorokhov, I.M., Semikhatov, M.A., Mel'nikov, N.N., Kozlov, V.I., 1997. Strontium isotopic composition in the limestones of the Inzer Formation, Upper Riphean Type Section, Southern Urals. Trans. (Doklady) Russ. Acad. Sci. (Earth Sci. Sect.) 353, 319–324.

Laird, M.G., 1981. In: Holland, C.H. (Ed.), Lower Palaeozoic of the Middle East, Eastern and Southern Africa, and Antarctica. John Wiley, Chichester.

Lee, J.Y., Marti, K., Severinghaus, K., Kawamura, K., Yoo, H.S., Lee, J.B., Kim, J.S., 2006. A redetermination of the isotopic abundances of atmospheric Ar. Geochim. Cosmochim. Acta 70, 4507–4512.

Lehmann, B., Nägler, T.F., Holland, H.D., Wille, M., Mao, J., Pan, J., Ma, D., Dulski, P., 2007. Highly metalliferous carbonaceous shale and Early Cambrian seawater. Geology 35, 403–406.

Lindgren, W., 1926. Ore Deposits of the Jerome and Bradshaw Mountains Quadrangles, Arizona. U.S. Geological Survey Bulletin 782.

Maloof, A.C., Porter, S.M., Moore, J.L., Dudás, F.Ö., Bowring, S.A., Higgins, J.A., Fike, D.A., Eddy, M.P., 2010. The earliest Cambrian record of animals and ocean geochemical change. Geol. Soc. Am. Bull. 122, 1731–1774.

Mancuso, J.J., Frizado, J.P., Schick, C.W., 1985. Unconformity-type uranium mineralization, central Dickinson County, Michigan. In: Institute on Lake Superior Geology, 34th Annual Meeting, Kenora, Ontario, Abstracts, 52.

Marchand, J., Bossière, G., Leyreloup, A., 1982. Pinite and pseudo-"glass" in high-grade metamorphic gneisses. Contrib. Miner. Petrol. 79, 439–442.

Mark, D.F., Parnell, J., Kelley, S.P., Sherlock, S.C., 2007. Resolution of regional fluid flow related to successive orogenic events on the Laurentian margin. Geology 35, 547–550.

Mark, D.F., Barfod, D.N., Stuart, F.M., Imlach, J.G., 2009. The ARGUS multicollector noble gas mass spectrometer: performance for $^{40}Ar/^{39}Ar$ geochronology. Geophys. Geochem. Geosyst. 10 (2), 1–9.

Mark, D.F., Rice, C.M., Fallick, A.E., Trewin, N.H., Lee, M.R., Boyce, A., Lee, J.K.W., 2011a. $^{40}Ar/^{39}Ar$ dating of hydrothermal activity, biota and gold mineralization in the Rhynie hot-spring system, Aberdeenshire, Scotland. Geochim. Cosmochim. Acta 75, 555–569.

Mark, D.F., Stuart, F.M., de Podesta, M., 2011b. New high-precision measurements of the isotopic composition of atmospheric argon. Geochim. Cosmochim. Acta 75, 7494–7501.

Mark, D.F., Patraglia, M., Smith, V., Morgan, L., Barfod, D., Ellis, B., Pearce, N., Pal, J.N., Korisettar, R., 2014. A high-precision $^{40}Ar/^{39}Ar$ age for the Young Toba Tuff and dating of ultra-distal tephra: forcing of Quaternary climate and implications for hominin occupation of India. Quater. Geochronol., http://dx.doi.org/10.1016/j.quageo.2012.12.004 (in press).

May, E.R., Dinkowitz, S.R., 1996. An overview of the Flambeau supergene enriched massive sulfide deposit: geology and mineralogy, Rusk County, Wisconsin. In: LaBerge, G.L. (Ed.), Proceedings of Volcanogenic Massive Sulfide Deposits of Northern Wisconsin, vol. 42 Part 2. Institute of Lake Superior Geology, pp. 67–93.

McIlroy, D., Brasier, M.D., Moseley, J.B., 1998. The Proterozoic-Cambrian transition within the 'Charnian Supergroup' of central England and the antiquity of the Ediacara fauna. J. Geol. Soc., Lond. 155, 401–411.

Morag, N., Avigad, D., Gerdes, A., Belousova, E., Harkavan, Y., 2011. Detrital zircon Hf isotopic composition indicates long-distance transport of North Gondwana Cambrian-Ordovician sandstones. Geology 39, 955–958.

Murphy, J.E., Ohle, E.L., 1968. The iron mountain mine, Iron Mountain, Missouri. In: Ridge, J.D. (Ed.), Ore Deposits of the United States, 1933–1967. The American Institute of Mining, Metallurgical, and Petroleum Engineers, Inc., New York, pp. 287–302.

Nazarov, M.A., Barsukova, L.D., Kolesov, G.M., Alekseev, A.S., 1983. Iridium abundances in the Precambrian–Cambrian boundary deposits and sedimentary rocks of Russian Platform. Lunar Planet. Sci. XIV, 546–547.

Nielsen, A.T., Schovsbo, N.H., 2011. The lower Cambrian of scandinavia: depositional environment, sequence stratigraphy and palaeogeography. Earth-Sci. Rev. 107, 207–310.

O'Brien, S.J., 2002. A note on Neoproterozoic gold, early Paleozoic copper and basement-cover relationships on the margins of the Holyrood Horst, southeastern Newfoundland. Current Research Newfoundland Department of Mines and Energy Geological Survey Report 02-1., pp. 219–227.

O'Hara, M.J., 1961. Zoned ultrabasic and basic gneiss masses in the early Lewisian metamorphic complex at Scourie, Sutherland. J. Petrol. 2, 248–276.

Paterson, C.J., Lisenbee, A.L., Redden, J.A., 1988. Gold deposits in the Black Hills, South Dakota. Wyo. Geol. Assoc. Guidebook 39, 295–304.

Peach, B.N., Horne, J., Gunn, W., Clough, C.T., Hinxman, L.W., 1907. The Geological Structure of the North-West Highlands of Scotland. Memoirs of the Geological Survey of Great Britain, HMSO, Glasgow.

Pelechaty, S.M., Grotzinger, J.P., Kashirtsev, V.A., Zhernovsky, V.P., 1996. Chemostratigraphic and sequence stratigraphic constraints on Vendian-Cambrian basin dynamics, northeast Siberian craton. J. Geol. 104, 543–563.

Pérez-García, L.C., Sánchez-Palencia, F.J., Torres-Ruiz, J., 2000. Tertiary and Quaternary alluvial gold deposits of Northwest Spain and Roman mining (NW of Duero and Bierzo Basins). J. Geochem. Explor. 71, 225–240.

Peters, S.E., Gaines, R.R., 2012. Formation of the 'Great Unconformity' as a trigger for the Cambrian explosion. Nature 484, 363–366.

Renne, P.R., Swisher, C.C., Deino, A.L., Karner, D.B., Owens, T.L., DePaolo, D.J., 1998. Intercalibration of standards, absolute ages and uncertainties in $^{40}Ar/^{39}Ar$ dating. Chem. Geol. 145, 117–152.

Renne, P.R., Deino, A.L., Hames, W.E., Heizler, M.T., Hemming, S.R., Hodges, K.V., Koppers, A.A.P., Mark, D.F., Morgan, L.E., Phillips, D., Singer, B.S., Turrin, B.D., Villa, I.M., Villeneuve, M., Wijbrans, J.R., 2009. Data reporting norms for $^{40}Ar/^{39}Ar$ geochronology. Quater. Geochronol. 4, 346–352.

Renne, P.R., Mundil, R., Balco, G., Min, K., Ludwig, K.R., 2010. Joint determination of ^{40}K decay constants and $^{40}Ar^*/^{40}K$ for the Fish Canyon sanidine standard, and improved accuracy for $^{40}Ar/^{39}Ar$ geochronology. Geochim. Cosmochim. Acta 74, 5349–5367.

Renne, P.R., Balco, G., Ludwig, K.R., Mundil, R., Min, K., 2011. Response to the comment by W.H. Schwarz et al. on 'Joint determination of 40K decay constants and 40K*/40K for the Fish Creek sanidine standard, and improved accuracy for $^{40}Ar/^{39}Ar$ geochronology' by P. R. Renne et al. (2010). Geochim. Cosmochim. Acta 75, 5097–5100.

Renne, P.R., Deino, A.L., Hilgen, F.J., Kuiper, K.F., Mark, D.F., Mitchell III, W.S., Morgan, L.E., Mundil, R., Smit, J., 2013. Time scales of critical events around the Cretaceous-Paleogene boundary. Science 339, 684–687.

Rivera, T.A., Storey, M., Zeeden, C., Hilgen, F.J., Kuiper, K., 2011. A refined astronomically calibrated $^{40}Ar/^{39}Ar$ age for Fish Canyon sanidine. Earth Planet. Sci. Lett. 311, 420–426.

Rogers, M.C., 2011. Saskatchewan descriptive mineral deposit models. Saskatchewan Geological Survey Open File Report 2011-57.

Russell, M.J., Allison, I., 1985. Agalmatolite and the maturity of sandstones of the Appin and Argyll Groups and Eriboll Sandstone. Scot. J. Geol. 21, 113–122.

Saskatchewan Ministry of Energy and Resources, 2008. Mineral Exploration Map of Saskatchewan.

Schoenberg, R., Zink, S., Staubwasser, M., von Blanckenburg, F., 2008. The stable Cr isotope inventory of solid Earth reservoirs determined by double spike MC-ICP-MS. Chem. Geol. 249, 294–306.

Schrödinger, S., Grotzinger, J.P., 2007. Evidence for anoxia at the Ediacaran-Cambrian boundary: the record of redox-sensitive trace elements and rare earth elements in Oman. J. Geol. Soc., London 164, 175–187.

Schwartz, G.M., 1938. Oxidized copper ores of the United Verde Extension Mine. Econ. Geol. 33, 21–33.

Shields, G., 1999. Working towards a new stratigraphic calibration scheme for the Neoproterozoic-Cambrian. Eclogae Geol. Helv. 92, 221–223.

Shields, G.A., 2007. A normalized seawater strontium isotope curve: possible implications for Neoproterozoic-Cambrian weathering rates and the further oxygenation of the Earth. eEarth 2, 35–42.

Simpson, E.L., Dilliard, K.A., Rowell, B.F., Higgins, D., 2002. The fluvial-to-marine transition within the post-rift Lower Cambrian Hardyston Formation, Eastern Pennsylvania, USA. Sediment. Geol. 147, 127–142.

Sinclair, I.G.L., Gasparrini, E., 1980. Textural features and age of supergene mineralization in the Detour copper–zinc–silver-deposit, Quebec. Econ. Geol. 75, 470–477.

Steiger, R.H., Jäger, E., 1977. Subcommission on geochronology: convention on the use of decay constants in geo- and cosmochronology. Earth Planet. Sci. Lett. 36, 359–362.

Thomas, C.W., 1999. The Petrology and Isotope Geochemistry of Dalradian Carbonate Rocks (Ph.D. thesis). University of Edinburgh, Edinburgh.

Torsvik, T.H., Smethurst, M.A., Meert, J.G., Van Der Voo, R., McKerrow, W.S., Brasier, M.D., Sturt, B.A., Walderhaug, H.J., 1996. Continental break-up and collision in the Neoproterozoic and Palaeozoic – a tale of Baltica and Laurentia. Earth-Sci. Rev. 40, 229–258.

Trinquier, A., Birck, J.L., Allegre, J.C., 2008. High-precision analysis of chromium isotopes in terrestrial and meteorite samples by thermal ionization mass spectrometry. J. Anal. Atom. Spectrom. 23, 1557–1696.

VanLaningham, S., Mark, D.F., 2011. Step-heating of $^{40}Ar/^{39}Ar$ standard mineral mixtures: investigation of a fine-grained bulk sediment provenance tool. Geochim. Cosmochim. Acta 75 (9), 2324–2335.

Walls, R.A., Ragland, P.C., Crisp, E.L., 1977. Experimental and natural early diagenetic mobility of Sr and Mg in biogenic carbonates. Geochim. Cosmochim. Acta 41, 1731–1737.

Weaver, B.L., Tarney, J., 1981. Lewisian gneiss geochemistry and Archean crustal development models. Earth Planet. Sci. Lett. 55, 171–180.

Wille, M., Nagler, T.F., Lehmann, B., Schroder, S., Kramers, J.D., 2008. Hydrogen sulphide release to surface waters at the Precambrian/Cambrian boundary. Nature 453, 767–769.

Xu, D., Zhang, Q., Sun, Y., Yan, Z., Chai, Z., He, J., 1989. The Precambrian–Cambrian boundary event. In: Astrogeological Events in China. Scottish Academic Press, Edinburgh.